Available online at www.sciencedirect.com
SCIENCE DIRECT®
Journal of Chromatography A, 987 (2003) 3–15
JOURNAL OF CHROMATOGRAPHY A
www.elsevier.com/locate/chroma

Thermodynamics and kinetics of solute transfer in reversed-phase liquid chromatography

Victoria L. McGuffin*, Chomin Lee
Department of Chemistry, 320 Chemistry Building, Michigan State University, East Lansing, MI 48824-1322, USA

Abstract

In this study, the thermodynamic and kinetic behavior of a homologous series of fatty acids is examined using a polymeric octadecylsilica stationary phase and a methanol mobile phase. The zone profiles are evaluated as the temperature is varied from 20 to 60 °C and the average pressure from 400 to 4570 p.s.i. (1 p.s.i.=6894.76 Pa). The rate constant for solute transfer from mobile to stationary phase (k_{ms}) appears to be relatively constant with carbon number. In contrast, the rate constant from stationary to mobile phase (k_{sm}) decreases logarithmically with increasing carbon number. This suggests that the mass transport processes become progressively slower, owing to the smaller diffusion coefficients of the larger solutes in the stationary phase. The activation energy decreases slightly in the mobile phase and increases slightly in the stationary phase with increasing carbon number. The activation energy in the stationary phase ranges from 41.6 to 55.9 kcal/mol, while the thermodynamic change in internal energy ranges from −9.8 to −29.0 kcal/mol for C_{10} to C_{22}, respectively (1 cal=4.184 J). The activation volume increases with increasing carbon number in both the mobile and stationary phase. The activation volume in the stationary phase ranges from 31.7 to 211 cm^3/mol, while the thermodynamic change in molar volume ranges from −27.1 to −104 cm^3/mol for C_{10} to C_{22}, respectively. These large changes in activation energy and volume suggest that the solutes do not enter and leave the stationary phase in a single step, but in a stepwise or progressive manner.

Keywords: Thermodynamic parameters; Kinetic studies; Solute transfer; Liquid chromatography; Rate constant; Activation energy; Activation volume; Molar internal energy; Molar volume; Retention mechanism; Fatty acids

1. Introduction

Octadecylsilica materials are the most common stationary phases for reversed-phase liquid chromatography [1–3]. Owing to the popularity of these materials, numerous studies have been conducted to investigate the influence of silica structure [4–10], bonding chemistry [11–18], temperature [13,19–23], pressure [24–27], and mobile phase composition [18,20,28–33] on chromatographic behavior. Although the thermodynamic properties of these materials have been studied for many years, the kinetic properties have not been fully elucidated. A deep understanding of the kinetic properties is essential to identify the rate-limiting processes so that separation speed may be increased without sacrificing efficiency.

There are several methods by which the kinetics of chromatographic interactions have been measured. For very fast interactions, spectroscopic methods such as fluorescence time decay or correlation techniques have been employed [34–36]. In general, these methods allow time resolution at the nanosecond level, which is too fast to follow the

*Corresponding author. Tel.: +1-517-355-9715x244; fax: +1-517-353-1793.
E-mail address: jgshabus@aol.com (V.L. McGuffin).

0021-9673/02/$ – see front matter
PII: S0021-9673(02)01455-3

typical rates of chromatographic processes. For intermediate interactions at the microsecond to millisecond level, relaxation methods such as temperature-jump [37–39], pressure-jump [39–41], or photon-induced dipole-jump [42] are useful. In these methods, the equilibrium distribution of the solute between the mobile and stationary phases is perturbed and the relaxation of the system to the new equilibrium state is then monitored by an appropriate detection method. However, because of the perturbation, this method inherently changes the equilibrium and kinetic behavior of the system that is being measured. Finally, slow interactions at the millisecond to second level may be monitored by means of chromatographic or other flow methods [43–54]. In these methods, the zone profiles are analyzed to determine plate heights, statistical moments, or other fitting parameters that are related to the rate constants for mass transport. The problems and inaccuracies associated with this method have been discussed by Weiss [55] and by Lenhoff [56]. Among these problems, there are many processes that contribute to the broadening and asymmetry of the zone profile that do not arise from kinetic sources. If these sources cannot be accurately measured or estimated, the resulting kinetic data will be in error.

To overcome this problem, a novel experimental system has been developed in our laboratory that permits examination of the solute zone profile at several points along an optically transparent capillary column. Because the retention measurements are made in situ, errors that arise from external sources are eliminated. Any change in the zone profile that arises between the detectors must be directly attributable to solute interactions with the mobile and stationary phases. Consequently, retention can be measured with very high accuracy and precision [24–26]. This system allows, for the first time, simultaneous determination of thermodynamic and kinetic information from a single study so that the results are internally consistent. Thermodynamic parameters, such as the retention factor and the associated changes in molar internal energy and molar volume, provide detailed information about the equilibrium or steady-state behavior. Kinetic parameters, such as the rate constants and the associated activation energy and volume, provide information about the nonequilibrium behavior. This information will provide a more thorough and detailed evaluation of the retention mechanism in reversed-phase liquid chromatography.

2. Experimental

2.1. Reagents

The saturated, even-numbered fatty acids (Sigma, St Louis, MO, USA) ranging from C_{10} to C_{22} are derivatized with 4-bromomethyl-7-methoxycoumarin as described previously [57]. The solvent is evaporated in a stream of dry nitrogen at 40 °C and the residue is redissolved in methanol at a final concentration of 10^{-4} *M*. All organic solvents are high-purity, spectroscopic grade (Honeywell Burdick & Jackson, Muskegon, MI, USA).

2.2. Chromatographic system

The stationary phase is prepared using an irregular silica material with particle size of 5.5 μm, pore size of 190 Å, and surface area of 240 m^2/g (IMPAQ 200, PQ Corp., Conshohocken, PA, USA). This material is reacted with trichlorooctadecylsilane in the presence of trace water to produce a polymeric phase with a bonding density of 5.4 $\mu mol/m^2$ [58,59]. The microcolumns are fabricated from 200 μm I.D. fused-silica capillary tubing (Polymicro Technologies, Phoenix, AZ, USA), terminated with a quartz wool frit at a length of 76.0 cm. The polyimide coating is removed from the capillary at distances of 23.2, 28.7, 52.8, and 58.3 cm to facilitate on-column detection. A 0.25-g sample of the octadecylsilica material is suspended in 1.0 ml methanol. This slurry is introduced onto the capillary at 5000 p.s.i., maintained at this pressure for 2 h, and then gradually reduced to 1000 p.s.i. for at least 10 h (1 p.s.i.=6894.76 Pa). The resulting microcolumn is evaluated under standard test conditions [60] to have a plate height of 15 μm, total porosity of 0.84, and flow resistance parameter of 500.

The experimental system has been described in previous work [26]. The methanol mobile phase is delivered by a single-piston reciprocating pump (Model 114M, Beckman Instruments, San Ramon,

CA, USA), operated in the constant-pressure mode (±15 p.s.i.). The sample is introduced by means of a 1.0-μl injection valve (Model ECI4W1, Valco Instruments, Houston, TX, USA) and is subsequently split between the microcolumn and a 50 μm I.D. fused-silica capillary (Polymicro Technologies), resulting in an injection volume of 12 nl. A 20 μm I.D. fused-silica capillary (Polymicro Technologies) is attached at the column outlet to serve as a restrictor. The column, injector, splitter and restrictor are maintained at constant temperature (±0.1 °C) in a cryogenically cooled oven (Model 3300, Varian Associates, Sugar Land, TX, USA).

The experiments are conducted by systematically changing either pressure or temperature, while maintaining all other factors constant. For the pressure studies, the lengths of the restricting and splitting capillaries are proportionally decreased, so that the mobile-phase linear velocity (0.08 cm/s at room temperature) and split ratio (1:84) remain constant as the inlet pressure is reduced from 5000 to 830 p.s.i. As the temperature is decreased from 60 to 20 °C, however, the linear velocity is allowed to change as a consequence of the variation in mobile-phase viscosity with temperature. In this manner, the pressure drop along the column is maintained constant at 800 p.s.i. throughout the experiments. The local pressure at each detection position is then calculated by assuming a linear pressure drop (11 p.s.i./cm) along the column. This calculation is verified by comparison with a more rigorous theoretical equation that accommodates the change in compressibility and viscosity of the mobile phase with both temperature and pressure [61,62]. The deviation between the values calculated with the assumption of linear pressure and with the more rigorous nonlinear equation is found to be less than 1.4% for the experimental conditions of this study.

2.3. Detection system

A laser-induced fluorescence detection system is used to examine the solute zones at four positions along the microcolumn. A continuous-wave He–Cd laser (Model 3074-20M, Omnichrome, Chino, CA, USA), with approximately 15 mW of power at 325 nm, is used as the excitation source. The laser radiation is transmitted to the microcolumn via small-diameter, UV-grade optical fibers (100 μm, Polymicro Technologies), and fluorescence emission is collected in a right-angle geometry using optical fibers of larger diameter (500 μm, Polymicro Technologies). The fluorescence emission at each detection position is isolated by an interference filter at 420 nm (Corion, Holliston, MA, USA) and is detected by a photomultiplier tube (Model R760, Hamamatsu, Middlesex, NJ, USA). The resulting photocurrent is amplified (100 nA/V, 0.01 s time constant) and converted to the digital domain (Model 3405/5716, Data Translation, Marlborough, MA, USA). Data acquisition is carried out using the Forth-based programming language Asyst (Version 2.1, Keithley Asyst, Rochester, NY, USA) with a personal computer. An acquisition rate of 1–5 Hz is employed to provide a minimum of 50 data points uniformly distributed across the solute zone profile.

2.4. Calculations

To characterize the thermodynamic and kinetic behavior, the solute zone profiles are analyzed by nonlinear regression (Version 3.18, Peakfit, SYSTAT Software, Richmond, CA, USA) using an exponentially modified Gaussian (EMG) equation:

$$C(t) = \frac{A}{2\tau} \cdot \exp\left[\frac{\sigma_G^2}{2\tau^2} + \frac{t_G - t}{\tau}\right] \cdot \left[\mathrm{erf}\left(\frac{t - t_G}{\sqrt{2}\,\sigma_G} - \frac{\sigma_G}{\sqrt{2}\,\tau}\right) + 1\right] \quad (1)$$

where $C(t)$ is the concentration as a function of time, A is the area, t_G is the retention time of the Gaussian component, σ_G^2 is the variance of the Gaussian component, and τ^2 is the variance of the exponential component [63,64]. The regression of the zone profiles to this equation is excellent, with typical values for the square of the correlation coefficient (r^2) of 0.99 or greater. Other equations of kinetic origin, specifically the Giddings equation [65], the Haarhoff–Van der Linde equation [66], and the nonlinear chromatography equation [46,67], do not fit well to the experimental data and evince nonrandom residuals. Moreover, the use of the EMG equation avoids the errors inherent in statistical moments [56,68].

The parameters of the EMG equation can be used to calculate the solute retention factor (k):

$$k = \frac{t_G + \tau - t_{G,0}}{t_{G,0}} \quad (2)$$

where $t_{G,0}$ is the Gaussian component of a non-retained peak. In previous studies, we have demonstrated that the retention factor remains constant with column length for the homologous series of fatty acids [68]. This confirms that the thermodynamic properties have achieved steady state. The retention factor is related to the changes in molar enthalpy (ΔH°) and molar entropy (ΔS°) in the following manner:

$$\ln k = \frac{-\Delta H^\circ + T\Delta S^\circ}{RT} + \ln \beta \quad (3)$$

where β is the volume ratio of the mobile and stationary phases. The change in molar enthalpy can be determined from the slope of a graph of the logarithm of the retention factor versus the inverse temperature ($1/T$) [25,26]. From the definition of the molar enthalpy [69],

$$\Delta H^\circ = \Delta E^\circ + P\Delta V^\circ \quad (4)$$

where ΔE° and ΔV° are the changes in molar internal energy and molar volume, respectively. By substitution in Eq. (3),

$$\ln k = \frac{-\Delta E^\circ - P\Delta V^\circ + T\Delta S^\circ}{RT} + \ln \beta \quad (5)$$

Thus, the change in molar volume can be determined from the slope of a graph of the logarithm of the retention factor versus the pressure (P) [25,26]. These thermodynamic properties provide detailed information about the solute transition between the mobile and stationary phases, which characterize the retention mechanism.

The other parameters of the EMG equation can be used to characterize the kinetic behavior of the system. In previous studies, we have demonstrated that the variance of the Gaussian and exponential components increases linearly with column length for the homologous series of fatty acids [68]. This confirms that the symmetric and asymmetric broadening arises from the column itself, rather than from extracolumn sources, and that this broadening is at steady state. The symmetric broadening arises from diffusion, multiple paths, and mass transport in the mobile and stationary phases that is rapid compared to the rate of solute migration through the column. The asymmetric broadening arises from slow mass transport kinetics, which is related to the rate constants for solute transfer from mobile to stationary phase (k_{ms}) and from stationary to mobile phase (k_{sm}).

$$k_{ms} = \frac{2k^2 t_{G,0}}{\tau^2} \quad (6)$$

$$k_{sm} = \frac{2k t_{G,0}}{\tau^2} \quad (7)$$

These ‘‘lumped’’ rate constants may include the processes of restricted diffusion in pores, slow diffusion in the stationary phase, interfacial resistance to mass transfer, etc. The kinetic rate constants are related to the thermodynamic retention factor by:

$$k = \frac{k_{ms}}{k_{sm}} \quad (8)$$

Once the rate constants have been determined, they can be used to establish the activation energy from the Arrhenius equation [69,70]:

$$\ln k_{ms} = \ln A_{m\ddagger} - \frac{\Delta E_{m\ddagger}}{RT} \quad (9)$$

$$\ln k_{sm} = \ln A_{s\ddagger} - \frac{\Delta E_{s\ddagger}}{RT} \quad (10)$$

In these equations, $A_{m\ddagger}$ is the pre-exponential factor and $\Delta E_{m\ddagger}$ is the activation energy arising from the mobile phase to transition state, while $A_{s\ddagger}$ and $\Delta E_{s\ddagger}$ arise from the stationary phase to transition state. Thus, the activation energies may be determined from graphs of the logarithm of the rate constants k_{ms} and k_{sm} versus the inverse temperature.

The activation energy is equal to the internal (potential) energy plus a kinetic energy term (RT) [70]. By substitution from classical thermodynamics,

$$\ln k_{ms} = \ln A_{m\ddagger} - \frac{\Delta H_{m\ddagger} + RT - P\Delta V_{m\ddagger}}{RT} \quad (11)$$

$$\ln k_{sm} = \ln A_{s\ddagger} - \frac{\Delta H_{s\ddagger} + RT - P\Delta V_{s\ddagger}}{RT} \quad (12)$$

In these equations, $\Delta H_{m\ddagger}$ is the activation enthalpy and $\Delta V_{m\ddagger}$ is the activation volume arising from the

mobile phase to transition state, while $\Delta H_{s\ddagger}$ and $\Delta V_{s\ddagger}$ arise from the stationary phase to transition state. Thus, the activation volumes may be determined from graphs of the logarithm of the rate constants k_{ms} and k_{sm} versus the pressure. These kinetic properties provide detailed information about the solute transition between the mobile and stationary phases, which characterize the retention mechanism.

3. Results and discussion

The goal of the present study is to gain a more detailed understanding of the retention mechanism in reversed-phase liquid chromatography. As discussed previously [24–27], such experiments must be conducted in a rigorous and systematic manner to allow the results to be meaningful and to permit correlation with theoretical models. To achieve these goals, the thermodynamic and kinetic behavior is evaluated from measurements of solute retention that are carried out directly on the chromatographic column. These measurements are representative of small, isolated regions of the column, where temperature and pressure are maintained relatively constant, rather than an average over the entire column length. In addition, the on-column measurements of solute retention are implicitly corrected for changes in linear velocity, due to compressibility of the mobile phase, as well as for extra-column effects. Moreover, specific precautions are taken in choosing the mobile phase and model solutes for this study. The use of pure methanol rather than a premixed solvent can prevent any preferential accumulation of the mobile-phase components in the stationary phase, which may vary with temperature and pressure. The use of a homologous series of fatty acids as model solutes can provide a theoretically predictable and systematic means to control retention by altering the carbon number. The thermodynamic and kinetic behavior of these solutes is derived concurrently from the same experimental data in order to provide a holistic view of the retention mechanism in reversed-phase liquid chromatography.

3.1. Thermodynamic behavior

The retention of the homologous series of fatty acids is shown for varying temperature and constant pressure in Fig. 1. At all temperatures, the logarithm of the retention factor increases linearly with carbon number for C_{10} to C_{18} ($r^2 = 0.999$ to 1.000), as expected when each ethylene group contributes equally to the retention. However, a slight deviation from linearity is observed for C_{20} and C_{22} that is consistent with previous reports [3,26,71,72]. This nonlinearity is intuitively reasonable, as explained by Tchapla et al. [3,71], because the additional carbon atoms in the C_{20} and C_{22} solutes cannot be fully inserted into the octadecylsilica stationary phase. This leads to slightly less retention than expected for these solutes.

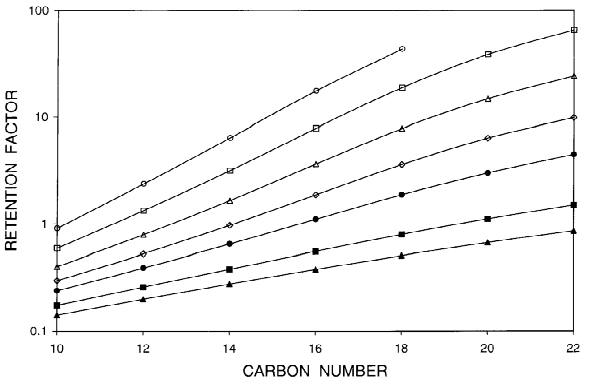

Fig. 1. Logarithm of the retention factor (k) versus carbon number for the homologous fatty acids. Temperature: (○) 20 °C, (□) 25 °C, (△) 30 °C, (◇) 35 °C, (●) 40 °C, (■) 50 °C, (▲) 60 °C. Pressure: 4570 p.s.i. Other experimental conditions as given in the text.

It is apparent from Fig. 1 that temperature has a significant effect on the retention. The retention factors for C_{10} to C_{22} decrease by 84.4 to 99.6%, respectively, as the temperature increases from 20 to 60 °C. The effect of temperature is much greater than generally observed for monomeric octadecylsilica stationary phases [13,21,30,73,74], but is consistent with the behavior of high-density polymeric phases. This effect is shown more clearly in Fig. 2, where the logarithm of the retention factor is graphed as a function of the inverse temperature. This Van 't Hoff plot is expected to be linear if the change in molar enthalpy is constant with temperature (Eq. (3)). This is clearly not the case, which is suggestive of a phase transition for this high-density octadecylsilica phase [26]. According to previous reports ([2] and refer-

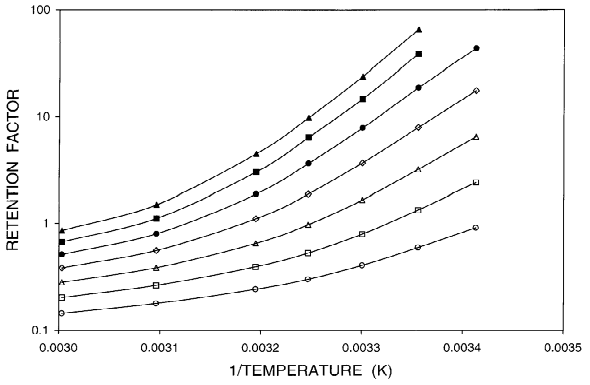

Fig. 2. Logarithm of the retention factor (k) versus inverse temperature ($1/T$) for the homologous fatty acids. Solutes: (○) C_{10}, (□) C_{12}, (△) C_{14}, (◇) C_{16}, (●) C_{18}, (■) C_{20}, (▲) C_{22}. Pressure: 4570 p.s.i. Other experimental conditions as given in the text.

ences cited therein), the phase transition of octadecylsilica materials is not a simple first-order phase transition but, instead, is more similar to order–disorder transitions for Langmuir–Blodgett monolayers [75]. At low temperatures, the ordered alkyl chain consists of all *trans* carbon–carbon bonds and, as temperature is increased, the degree of disorder is increased by *gauche* bonds. The disordering process is progressive, beginning at the distal end and gradually prevailing to the proximal group that is bound to the silica surface [76,77]. Because of the progressive nature of this phase transition, it does not occur at a single temperature like a first-order phase transition, but over a broader temperature range. For this high-density octadecylsilica phase, the transition occurs in the vicinity of 45 °C and extends over a range of approximately 20 °C. Above and below the transition temperature, the Van 't Hoff plot in Fig. 2 is relatively linear ($r^2=0.996$ to 1.000) and the change in molar enthalpy is constant [26]. From the molar enthalpy, the change in molar internal energy can be calculated according to Eq. (4). Representative values are summarized in Table 1 at 30 °C and 4570 p.s.i. It is apparent that the molar internal energy becomes systematically more negative, ranging from −9.8 to −29.0 kcal/mol for C_{10} to C_{22}, respectively (1 cal = 4.184 J). The differential change in molar internal energy per ethylene group ($\Delta\Delta E^\circ$) remains constant for solutes C_{10} to C_{18} at -3.5 ± 0.1

Table 1
Change in internal energy (ΔE°) and activation energies ($\Delta E_{m\ddagger}$ and $\Delta E_{s\ddagger}$) for retention of the homologous fatty acids in reversed-phase liquid chromatography

Solute	ΔE° (kcal/mol)	$\Delta E_{m\ddagger}$ (kcal/mol)	$\Delta E_{s\ddagger}$ (kcal/mol)
C_{10}	−9.8	26.6	41.6
C_{12}	−13.3	30.2	48.6
C_{14}	−16.7	28.4	49.3
C_{16}	−20.2	25.8	51.3
C_{18}	−23.9	24.3	53.6
C_{20}	−26.8	22.0	54.7
C_{22}	−29.0	19.3	55.9

Temperature: 30 °C; pressure: 4570 p.s.i. Other experimental conditions as given in the text.

kcal/mol. However, the solutes C_{20} and C_{22} have slightly smaller values of −2.9 and −2.2 kcal/mol, respectively. Again, these smaller internal energies are intuitively reasonable, as the additional carbon atoms cannot be fully inserted into the octadecylsilica stationary phase.

The retention of the homologous series of fatty acids is shown for varying pressure and constant temperature in Fig. 3. At all pressures, the logarithm of the retention factor is linearly related to carbon number for solutes C_{10} to C_{18} ($r^2=0.999$ to 1.000), but is slightly nonlinear for C_{20} and C_{22}. It is apparent that pressure also has a significant effect upon retention. The retention factors for C_{10} to C_{22} increase by 38.9 to 206%, respectively, as the

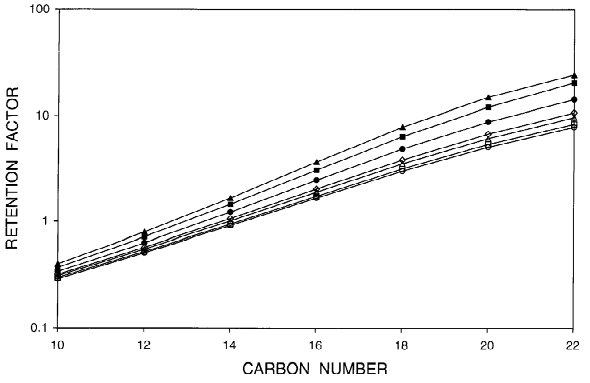

Fig. 3. Logarithm of the retention factor (k) versus carbon number for the homologous fatty acids. Temperature: 30 °C. Pressure: (○) 400 p.s.i., (□) 570 p.s.i., (△) 1070 p.s.i., (◇) 1470 p.s.i., (●) 2570 p.s.i., (■) 3570 p.s.i., (▲) 4570 p.s.i. Other experimental conditions as given in the text.

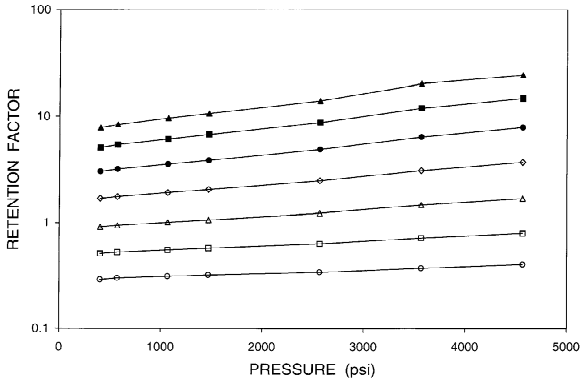

Fig. 4. Logarithm of the retention factor (k) versus pressure (P) for the homologous fatty acids. Solutes: (○) C_{10}, (□) C_{12}, (△) C_{14}, (◇) C_{16}, (●) C_{18}, (■) C_{20}, (▲) C_{22}. Temperature: 30 °C. Other experimental conditions as given in the text.

average pressure increases from 400 to 4570 p.s.i. Again, the effect of pressure is much greater than expected for monomeric octadecylsilica stationary phases [26,27], but is consistent with the behavior of high-density polymeric phases. This effect is shown more clearly in Fig. 4, where the logarithm of the retention factor is graphed as a function of the pressure. This plot is linear ($r^2=0.994$ to 0.999), as expected when the change in molar volume is constant with pressure (Eq. (5)). Representative values are summarized in Table 2 at 30 °C. It is apparent that the molar volume becomes systematically more negative, ranging from -27.1 to -104 cm^3/mol for C_{10} to C_{22}, respectively. These negative values imply that the solutes occupy less volume in the octadecylsilica stationary phase than in the methanol mobile phase. This conclusion is reasonable, since the similar structure of the solutes and stationary phase may allow for perfect alignment and, hence, a very close fit. The changes in molar volume are quite significant, typically 15 to 25% of the net volume of the alkyl chain. The differential change in molar volume per ethylene group ($\Delta\Delta V°$) remains constant for solutes C_{12} to C_{18} at -15.3 ± 1.4 cm^3/mol. However, the solutes C_{20} and C_{22} have slightly smaller values of -9.5 and -11.1 cm^3/mol, respectively. Again, these smaller volumes are intuitively reasonable, as the additional carbon atoms cannot be fully inserted into the octadecylsilica stationary phase.

3.2. Kinetic behavior

For consistency with the thermodynamic behavior, the kinetic behavior is elucidated from the same solute zone profiles according to Eqs. (6) and (7). The rate constants are shown in Fig. 5 and Table 3 at constant temperature and pressure. The rate constant from mobile to stationary phase (k_{ms}) decreases only slightly with carbon number, whereas the rate constant from stationary to mobile phase (k_{sm}) decreases by nearly three orders of magnitude. For solute C_{10}, the rate of mass transfer is limited by k_{ms}, whereas for solutes C_{12} to C_{22}, it is limited by k_{sm}. This is expected, according to Eq. (8), as the retention factor for C_{10} is less than unity whereas those for C_{12} to C_{22} are greater than unity at this temperature and pressure. The logarithm of the rate constants k_{ms} and k_{sm} appears to decrease linearly with carbon number for C_{10} to C_{18} ($r^2=0.974$ and 0.998, respectively). This suggests that each ethylene group has approxi-

Table 2
Molar volume (V), change in molar volume ($\Delta V°$), and activation volumes ($\Delta V_{m‡}$ and $\Delta V_{s‡}$) for retention of the homologous fatty acids in reversed-phase liquid chromatography

Solute	V (cm^3/mol)	$\Delta V°$ (cm^3/mol)	$\Delta V_{m‡}$ (cm^3/mol)	$\Delta V_{s‡}$ (cm^3/mol)
C_{10}	201	−27.1	7.2	31.7
C_{12}	241	−37.4	55.3	91.4
C_{14}	281	−51.7	64.8	116
C_{16}	321	−68.6	79.3	147
C_{18}	361	−83.4	87.1	171
C_{20}	401	−92.9	93.4	179
C_{22}	441	−104	110	211

Molar volume estimated by the method of Le Bas [78]. Temperature: 30 °C. Other experimental conditions as given in the text.

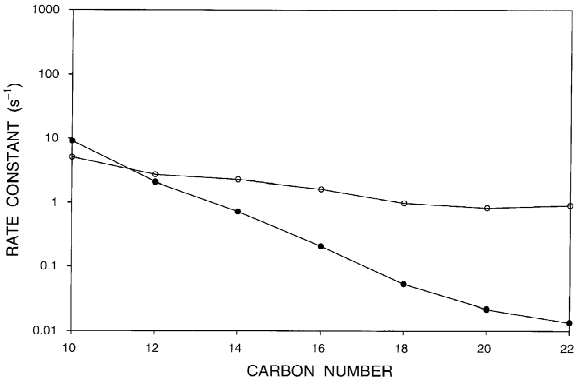

Fig. 5. Logarithm of the rate constants k_{ms} (○) and k_{sm} (●) versus carbon number for the homologous fatty acids. Temperature: 25 °C. Pressure: 4570 p.s.i. Other experimental conditions as given in the text.

mately an equal contribution to the kinetic behavior, just as it does for the thermodynamic behavior. Also similar to the thermodynamic behavior, there appears to be a slight nonlinearity for C_{20} and C_{22}. From the rate constants k_{ms} and k_{sm}, the characteristic time (t) for residence in the stationary and mobile phases can be calculated:

$$t = \frac{1}{k_{ms} + k_{sm}} \tag{13}$$

As shown in Table 3, the mean residence time increases systematically from 0.07 to 0.97 s for C_{10} to C_{18}, but remains relatively constant at 1.18 and 1.09 s for C_{20} and C_{22}, respectively. This kinetic behavior is reasonable, as the additional carbon atoms cannot be fully inserted into the octadecylsilica stationary phase.

Table 3
Retention factor (k), rate constants (k_{ms} and k_{sm}), and characteristic time (t) for retention of the homologous fatty acids in reversed-phase liquid chromatography

Solute	k	k_{ms} (s^{-1})	k_{sm} (s^{-1})	t (s)
C_{10}	0.56	5.05	9.08	0.071
C_{12}	1.29	2.68	2.08	0.21
C_{14}	3.12	2.26	0.72	0.34
C_{16}	7.88	1.62	0.21	0.55
C_{18}	18.8	0.98	0.052	0.97
C_{20}	38.5	0.83	0.021	1.18
C_{22}	67.3	0.90	0.013	1.09

Temperature: 25 °C; pressure: 4570 p.s.i. Other experimental conditions as given in the text.

The logarithm of the rate constants is shown as a function of carbon number and temperature in Fig. 6. Below the transition temperature of 45 °C, the trend for k_{ms} and k_{sm} is similar to that shown in Fig. 5. When the stationary phase is in the ordered state, hindered diffusion influences the rate of mass transfer slightly from mobile to stationary phase and more significantly from stationary to mobile phase. Hence, both rate constants decrease systematically with carbon number. Above the transition temperature, however, the stationary phase becomes more disordered and diffusion is more facile. In this tempera-

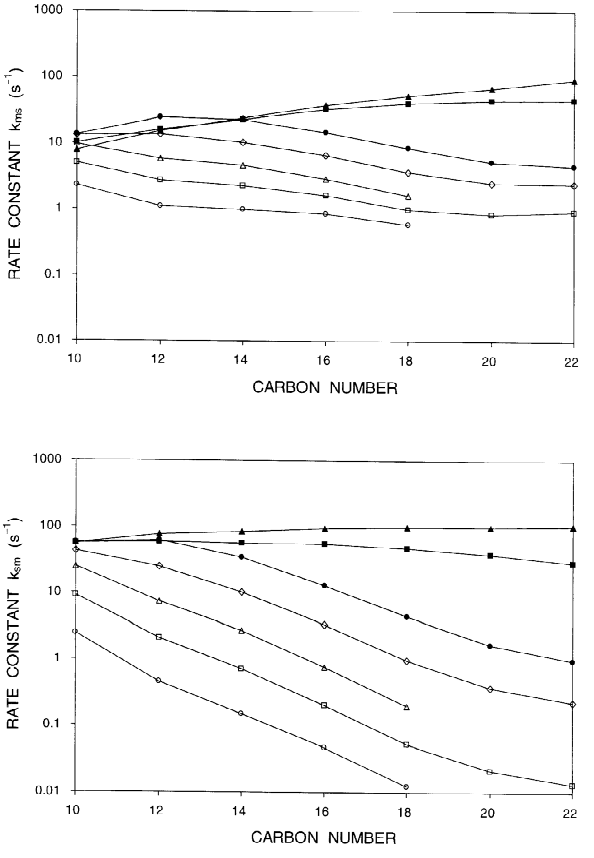

Fig. 6. Logarithm of the rate constants k_{ms} (top) and k_{sm} (bottom) versus carbon number for the homologous fatty acids. Temperature: (○) 20 °C, (□) 25 °C, (△) 30 °C, (◇) 35 °C, (●) 40 °C, (■) 50 °C, (▲) 60 °C. Pressure: 4570 p.s.i. Other experimental conditions as given in the text.

ture range, the rate of mass transfer is influenced more greatly by the attraction between solute and stationary phase. Hence, both rate constants increase systematically with carbon number.

As shown in Fig. 6, the rate constants increase systematically with temperature up to 45 °C, then become relatively constant. For a small solute such as C_{10}, k_{ms} increases by approximately one order of magnitude and k_{sm} by slightly more than one order of magnitude over the temperature range from 20 to 60 °C. For a large solute such as C_{22}, however, k_{ms} increases by more than two orders of magnitude and k_{sm} by more than four orders of magnitude. In order to investigate the source of these dramatic changes in the rate of mass transfer, it is useful to graph the logarithm of the rate constant as a function of the retention factor. As shown in Fig. 7, the change in retention factor of the fatty acids with temperature accounts for part but certainly not all of the observed change in rate constants. There remains an intrinsic dependence of the rate constants on temperature. For example, k_{ms} and k_{sm} increase from 1.85 to 118 s^{-1} as the temperature increases from 20 to 60 °C for a constant retention factor of 1.0. If we consider the simple ''rule of thumb'' [69,70], a 10 °C change in temperature would be expected to approximately double the rate constant. Thus, the observed 63-fold increase is larger than the expected 16-fold increase for a simple chemical reaction, undoubtedly owing to the phase transition that occurs at 45 °C.

A graph of the logarithm of the rate constants is shown as a function of the inverse temperature in Fig. 8. This Arrhenius plot is expected to be linear if the activation energy is constant with temperature (Eqs. (9) and (10)). This is clearly not the case because of the phase transition around 45 °C. Similar to the thermodynamic behavior in the Van 't Hoff plot (Fig. 2), the Arrhenius plot is relatively linear and the activation energy is constant above and below the transition temperature. Above the transition temperature, the slope is shallow and suggests that the activation energy is very small. Below the transition temperature, however, the slope is more substantial. Representative values are summarized in Table 1 at 30 °C and 4570 p.s.i. It is apparent that the activation energy from the mobile to stationary phase becomes systematically smaller, ranging from 30.2 to 19.3 kcal/mol for C_{12} to C_{22}, respectively. In

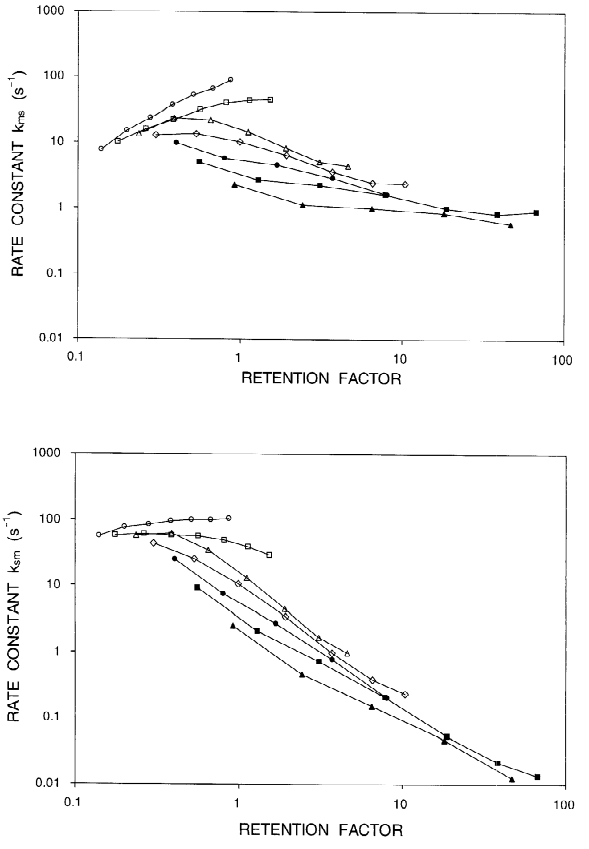

Fig. 7. Logarithm of the rate constants k_{ms} (top) and k_{sm} (bottom) versus retention factor (k) for the homologous fatty acids. Temperature: (○) 20 °C, (□) 25 °C, (△) 30 °C, (◇) 35 °C, (●) 40 °C, (■) 50 °C, (▲) 60 °C. Pressure: 4570 p.s.i. Other experimental conditions as given in the text.

contrast, the activation energy from stationary to mobile phase becomes systematically larger, ranging from 41.6 to 55.9 kcal/mol for C_{10} to C_{22}, respectively. These large activation energies suggest that the solutes do not enter and leave the stationary phase in a single step, but in a stepwise or progressive manner. The transport of an ethylene group would require only 1–3 kcal/mol, according to Table 1, which is energetically feasible within the chromatographic system.

The logarithm of the rate constants is shown as a function of carbon number and pressure in Fig. 9. At all pressures, the logarithm of the rate constants decreases linearly with carbon number for solutes C_{10} to C_{18} but is slightly nonlinear for C_{20} and C_{22}.

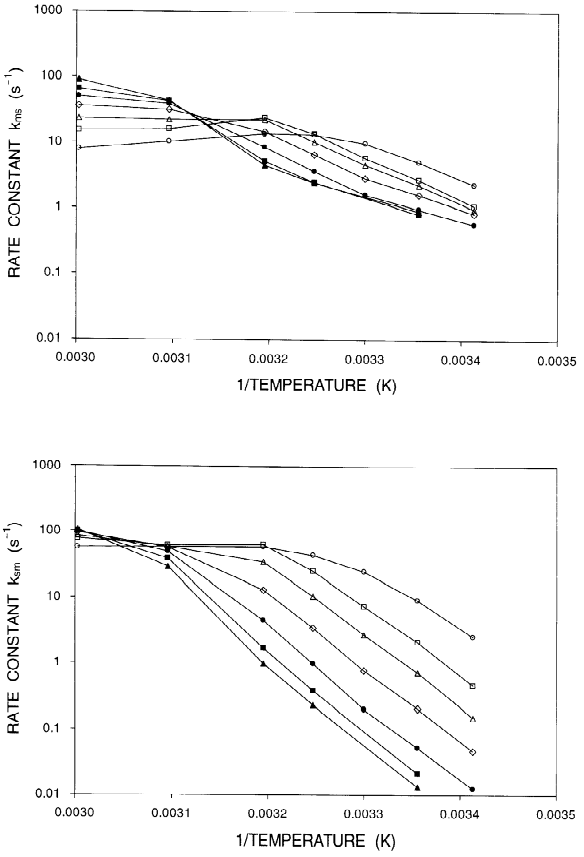

Fig. 8. Logarithm of the rate constants k_{ms} (top) and k_{sm} (bottom) versus inverse temperature ($1/T$) for the homologous fatty acids. Solutes: (○) C_{10}, (□) C_{12}, (△) C_{14}, (◇) C_{16}, (●) C_{18}, (■) C_{20}, (▲) C_{22}. Pressure: 4570 p.s.i. Other experimental conditions as given in the text.

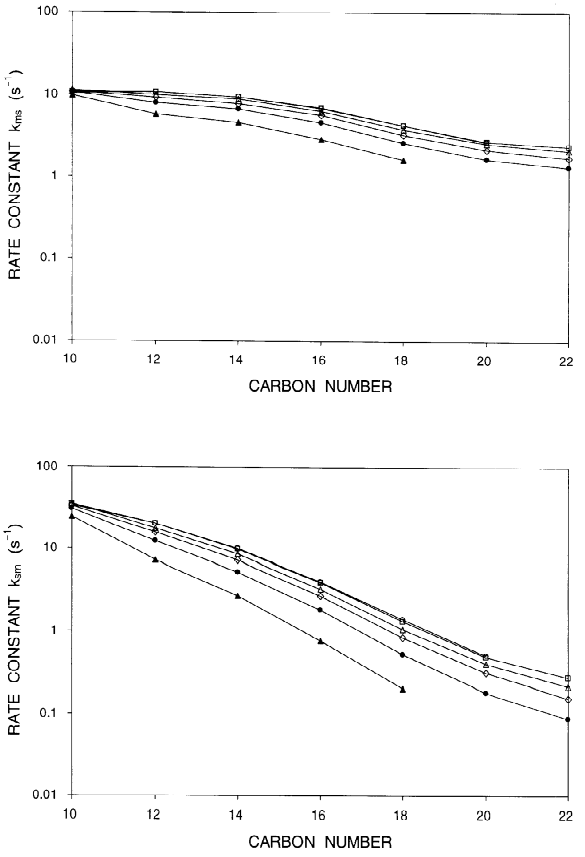

Fig. 9. Logarithm of the rate constants k_{ms} (top) and k_{sm} (bottom) versus carbon number for the homologous fatty acids. Temperature: 30 °C. Pressure: (○) 400 p.s.i., (□) 570 p.s.i., (△) 1070 p.s.i., (◇) 1470 p.s.i., (●) 2570 p.s.i., (▲) 4570 p.s.i. Other experimental conditions as given in the text.

For each solute, the rate constants decrease slightly with pressure. For a small solute such as C_{10}, k_{ms} decreases by 5% and k_{sm} by 30% over the pressure range from 400 to 4570 p.s.i. For a large solute such as C_{22}, however, k_{ms} and k_{sm} decrease by approximately an order of magnitude. To examine this effect in more detail, it is helpful to graph the logarithm of the rate constant as a function of the retention factor. As shown in Fig. 10, the change in retention factor of the fatty acids with pressure accounts for almost all of the observed change in rate constant. There remains only a small intrinsic dependence of the rate constants on pressure. For example, k_{ms} and k_{sm} decrease from 7.80 to 5.72 s^{-1} as the pressure increases from 400 to 4570 p.s.i. for a constant retention factor of 1.0. This represents a 27% decrease in the rate of transport for the fatty acids due to compression of the octadecylsilica stationary phase.

A graph of the logarithm of the rate constants is shown as a function of the pressure in Fig. 11. This plot is linear, as expected when the activation volume is constant with pressure (Eqs. (11) and (12)). Representative values are summarized in Table 2 at 30 °C. It is apparent that the activation volume from mobile to stationary phase becomes systematically larger, ranging from 55.3 to 110 cm^3/mol for C_{12} to C_{22}, respectively. The activation volume from stationary to mobile phase also becomes systematically larger, ranging from 91.4 to

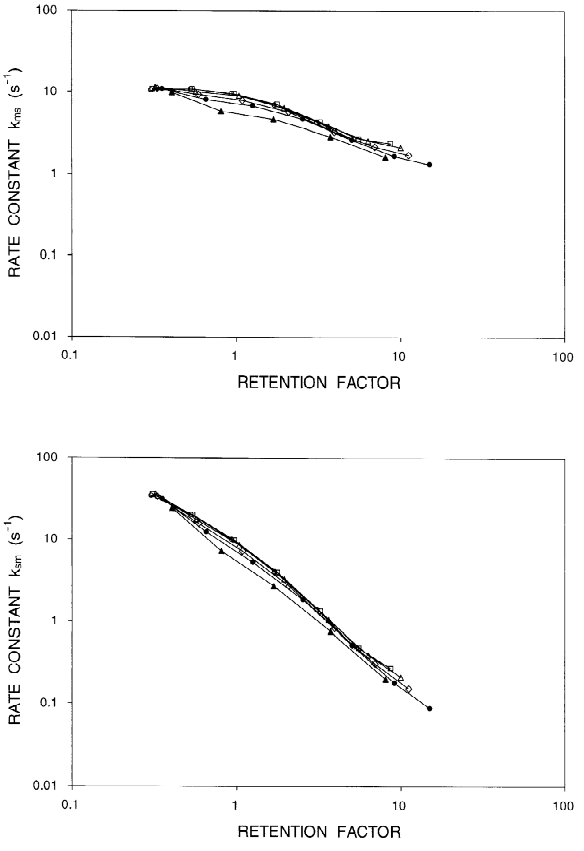

Fig. 10. Logarithm of the rate constants k_{ms} (top) and k_{sm} (bottom) versus retention factor (k) for the homologous fatty acids. Temperature: 30 °C. Pressure: (○) 400 p.s.i., (□) 570 p.s.i., (△) 1070 p.s.i., (◇) 1470 p.s.i., (●) 2570 p.s.i., (▲) 4570 p.s.i. Other experimental conditions as given in the text.

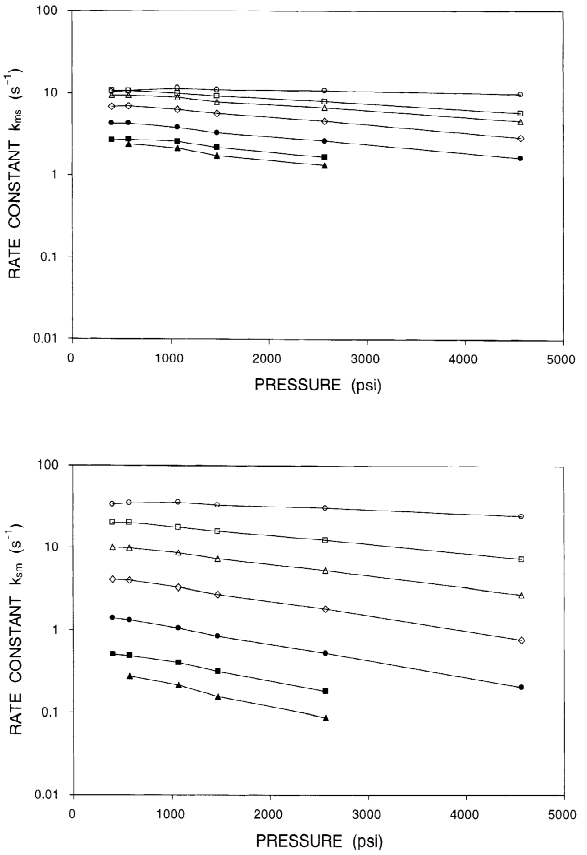

Fig. 11. Logarithm of the rate constants k_{ms} (top) and k_{sm} (bottom) versus pressure (P) for the homologous fatty acids. Solutes: (○) C_{10}, (□) C_{12}, (△) C_{14}, (◇) C_{16}, (●) C_{18}, (■) C_{20}, (▲) C_{22}. Temperature: 30 °C. Other experimental conditions as given in the text.

211 cm^3/mol for C_{12} to C_{22}, respectively. These activation volumes are quite significant, typically 25 to 50% of the net volume of the alkyl chain. These large activation volumes also suggest that the solutes do not enter and leave the stationary phase in a single step, but in a stepwise or progressive manner. The transport of an ethylene group would require 10–30 cm^3/mol, according to Table 2, which is volumetrically feasible within the chromatographic system.

3.3. Relationship between thermodynamic and kinetic behavior

Finally, it is beneficial to examine the relationship between the thermodynamic and kinetic behavior of the solutes. A priori, there is no expected relationship between the retention factor and the individual rate constants other than that given by Eq. (8). In practice, however, there are three cases that are commonly observed for a closely related series of solutes [70]. In the first limiting case, k_{sm} is constant and k is linearly related to k_{ms}. In the second limiting case, k_{ms} is constant and k is inversely related to k_{sm}. In the third case, which is relatively common, k varies with both k_{ms} and k_{sm} in a more complex manner. The data in Figs. 7 and 11 provide the first information about this relationship for reversed-phase liquid chromatography. At temperatures substantially below the phase transition, the system

behaves as the second limiting case where retention is primarily controlled by the rate constant from stationary to mobile phase. At temperatures above the phase transition, the system behaves as the first limiting case where retention is primarily controlled by the rate constant from mobile to stationary phase. At intermediate temperatures, however, retention is influenced in a substantive manner by both of these rate constants. When compared with temperature, pressure has much less effect on the relationship between thermodynamic and kinetic behavior.

4. Summary

In order to understand the implications of these results, it is helpful to follow the thermodynamic and kinetic behavior of a single solute. For example, as the C_{22} solute transfers from the mobile to stationary phase, it passes through a high-energy transition state. This transition state may be envisioned as a cavity created within the stationary phase that incorporates the solute as well as some associated solvent molecules. The creation of this transition state requires 19.3 kcal/mol and requires a volume that is 110 cm^3/mol or approximately 25% larger than the solute volume in the mobile phase. As mentioned previously, this large change in energy and volume suggests that the solute does not enter the stationary phase in a single step, but in a stepwise or progressive manner. As the system equilibrates, the solvent molecules are released and the alkyl chains of the stationary phase rearrange to accommodate and interact optimally with the solute. This involves a net stabilization energy of approximately -48.3 kcal/mol and a net decrease in volume of approximately -214 cm^3/mol. This transfer occurs with a rate constant of 0.90 s^{-1}. As the C_{22} solute transfers from the stationary to mobile phase, it passes through a high-energy transition state that may be similar but not necessarily identical to that described above. The creation of this transition state requires 55.9 kcal/mol and requires a volume that is 211 cm^3/mol or approximately 50% larger than the solute volume in the mobile phase. Again, this large change in energy and volume suggests that the solute does not leave the stationary phase in a single step, but in a stepwise or progressive manner. As the system equilibrates, the solute becomes solvated by the mobile phase and departs from the cavity in the stationary phase. Ultimately, the alkyl chains of the stationary phase rearrange and the cavity closes. This involves a net stabilization energy of approximately -26.9 kcal/mol and a net decrease in volume of approximately -107 cm^3/mol. This transfer occurs with a rate constant of 0.013 s^{-1}, which is 67-fold slower than the transfer from mobile to stationary phase.

This thermodynamic and kinetic information provides a detailed and holistic view of the retention mechanism in reversed-phase liquid chromatography. For the thermodynamic behavior, there are significant changes in retention factor and the associated molar internal energy and volume with temperature, pressure, and carbon number. For the kinetic behavior, there are significant changes in rate constant and the associated activation energy and volume with temperature, pressure, and carbon number. These changes are characteristic of the high-density, polymeric octadecylsilica material, but are likely to be much greater than monomeric and oligomeric phases. Moreover, these changes are characteristic of the fatty acid solutes, but are likely to be much greater than other solutes that are not templates of the stationary phase. More detailed studies of other stationary phases and other solutes will be necessary to provide a complete description of the retention mechanism in reversed-phase liquid chromatography.

Acknowledgements

The authors are grateful to Dr Lane C. Sander (National Institute of Standards and Technology) for synthesis of the octadecylsilica stationary phase and to Dr Shu-Hui Chen for acquisition of the experimental data.

References

[1] L.C. Sander, S.A. Wise, CRC Crit. Rev. Anal. Chem. 18 (1987) 299.
[2] J.F. Wheeler, T.L. Beck, S.J. Klatte, L.A. Cole, J.G. Dorsey, J. Chromatogr. A 656 (1993) 317.

[3] A. Tchapla, S. Heron, E. Lesellier, H. Colin, J. Chromatogr. A 656 (1993) 81.
[4] E.C. Nice, M.J. O'Hare, J. Chromatogr. 166 (1978) 263.
[5] K. Ogan, E. Katz, J. Chromatogr. 188 (1980) 115.
[6] R.J. Amos, J. Chromatogr. 204 (1981) 409.
[7] S.A. Wise, W.E. May, Anal. Chem. 55 (1983) 1479.
[8] L.C. Sander, S.A. Wise, Anal. Chem. 56 (1984) 504.
[9] J. Nawrocki, Chromatographia 31 (1991) 177.
[10] J. Nawrocki, Chromatographia 31 (1991) 193.
[11] R.K. Gilpin, M.F. Burke, Anal. Chem. 45 (1983) 1383.
[12] S.S. Yang, R.K. Gilpin, J. Chromatogr. 449 (1988) 115.
[13] L.A. Cole, J.G. Dorsey, Anal. Chem. 64 (1992) 1317.
[14] L.C. Tan, P.W. Carr, M. Abraham, J. Chromatogr. A 752 (1996) 1.
[15] J.H. Park, Y.K. Lee, Y.C. Weon, L.C. Tan, J. Li, L. Li, J.F. Evans, P.W. Carr, J. Chromatogr. A 767 (1997) 1.
[16] L.C. Tan, P.W. Carr, J. Chromatogr. A 775 (1997) 1.
[17] M. Reta, P.W. Carr, P.C. Sadek, S.C. Rutan, Anal. Chem. 71 (1999) 3484.
[18] R.P.J. Ranatunga, P.W. Carr, Anal. Chem. 72 (2000) 5679.
[19] D. Morel, J. Serpinet, J. Chromatogr. 248 (1982) 231.
[20] P.W. Carr, R.M. Doherty, M.J. Kamlet, R.W. Taft, W. Melander, Cs. Horváth, Anal. Chem. 58 (1986) 2674.
[21] A. Tchapla, S. Heron, H. Colin, G. Guiochon, Anal. Chem. 60 (1988) 1443.
[22] A. Tchapla, S. Heron, J. Chromatogr. A 684 (1994) 175.
[23] K.B. Sentell, N.I. Ryan, A.N. Henderson, Anal. Chim. Acta 307 (1995) 203.
[24] V.L. McGuffin, C.E. Evans, J. Microcol. Sep. 3 (1991) 513.
[25] V.L. McGuffin, C.E. Evans, S.H. Chen, J. Microcol. Sep. 5 (1993) 3.
[26] V.L. McGuffin, S.H. Chen, J. Chromatogr. A 762 (1997) 35.
[27] V.L. McGuffin, S.H. Chen, Anal. Chem. 69 (1997) 930.
[28] E.J. Kitka, E. Grushka, Anal. Chem. 48 (1976) 1098.
[29] L.C. Sander, L.R. Field, Anal. Chem. 52 (1980) 2009.
[30] A.M. Stalcup, D.L. Martire, S.A. Wise, J. Chromatogr. 442 (1988) 1.
[31] L.A. Cole, J.G. Dorsey, K.A. Dill, Anal. Chem. 64 (1992) 1324.
[32] A. Alvarez-Zepeda, B.N. Barman, D.E. Martire, Anal. Chem. 64 (1992) 1978.
[33] L.C. Tan, P.W. Carr, J. Chromatogr. A 799 (1998) 1.
[34] J.W. Carr, J.M. Harris, Anal. Chem. 59 (1987) 2546.
[35] R.L. Hansen, J.M. Harris, Anal. Chem. 70 (1998) 2565.
[36] R.L. Hansen, J.M. Harris, Anal. Chem. 70 (1998) 4247.
[37] S.W. Waite, D.B. Marshall, J.M. Harris, Anal. Chem. 66 (1994) 2052.
[38] F.Y. Ren, J.M. Harris, Anal. Chem. 68 (1996) 1651.
[39] J.M. Harris, D.B. Marshall, J. Microcol. Sep. 9 (1997) 185.
[40] D.B. Marshall, J.W. Burns, D.E. Connolly, J. Chromatogr. 360 (1986) 13.
[41] D.B. Marshall, J.W. Burns, D.E. Connolly, J. Am. Chem. Soc. 108 (1986) 1087.
[42] S.R. Shield, J.M. Harris, Anal. Chem. 74 (2002) 2248.
[43] C. Horvath, H. Lin, J. Chromatogr. 149 (1978) 43.
[44] F.H. Arnold, S.A. Schofield, H.W. Blanch, J. Chromatogr. 355 (1986) 1.
[45] F.H. Arnold, H.W. Blanch, J. Chromatogr. 355 (1986) 13.
[46] J.L. Wade, A.F. Bergold, P.W. Carr, Anal. Chem. 59 (1987) 1286.
[47] M.S. Uddin, K. Hidajat, C.B. Ching, Ind. Eng. Chem. Res. 29 (1990) 647.
[48] S. Golshan-Shirazi, G. Guiochon, J. Phys. Chem. 95 (1991) 6390.
[49] S. Golshan-Shirazi, G. Guiochon, J. Chromatogr. 603 (1992) 1.
[50] P.D. Munro, D.J. Winzor, J.R. Cann, J. Chromatogr. A 659 (1994) 267.
[51] J. Renard, C. Vidal-Madjar, J. Chromatogr. A 661 (1994) 35.
[52] D. Gowanlock, R. Bailey, F.F. Cantwell, J. Chromatogr. A 726 (1996) 1.
[53] J.Y. Li, L.M. Litwinson, F.F. Cantwell, J. Chromatogr. A 726 (1996) 25.
[54] J.Y. Li, F.F. Cantwell, J. Chromatogr. A 726 (1996) 37.
[55] G.H. Weiss, Sep. Sci. Technol. 16 (1981) 75.
[56] A.M. Lenhoff, J. Chromatogr. 384 (1987) 285.
[57] V.L. McGuffin, R.N. Zare, Appl. Spectrosc. 39 (1985) 847.
[58] L.C. Sander, S.A. Wise, Anal. Chem. 56 (1984) 504.
[59] L.C. Sander, National Institute of Standards and Technology, Gaithersburg, MD, personal communication, 1993.
[60] J.C. Gluckman, A. Hirose, V.L. McGuffin, M. Novotny, Chromatographia 17 (1983) 303.
[61] D.E. Martire, J. Chromatogr. 461 (1989) 165.
[62] S.H. Chen, Ph.D. Dissertation, Michigan State University, East Lansing, MI, 1993.
[63] J.P. Foley, J.G. Dorsey, J. Chromatogr. Sci. 22 (1984) 40.
[64] M.S. Jeansonne, J.P. Foley, J. Chromatogr. Sci. 29 (1991) 258.
[65] J.C. Giddings, Dynamics of Chromatography, Marcel Dekker, New York, 1965.
[66] P.C. Haarhoff, H.J. Van der Linde, Anal. Chem. 38 (1966) 573.
[67] H.C. Thomas, J. Am. Chem. Soc. 66 (1944) 1664.
[68] S.B. Howerton, C. Lee, V.L. McGuffin, Anal. Chim. Acta, in press.
[69] P.W. Atkins, Physical Chemistry, 6th ed., W.H. Freeman, New York, 1997.
[70] J.I. Steinfeld, J.S. Francisco, W.L. Hase, Chemical Kinetics and Dynamics, Prentice-Hall, Englewood Cliffs, NJ, 1989.
[71] A. Tchapla, H. Colin, G. Guiochon, Anal. Chem. 56 (1984) 621.
[72] S. Heron, A. Tchapla, Chromatographia 36 (1993) 11.
[73] L.R. Snyder, J. Chromatogr. 179 (1979) 167.
[74] D. Morel, J. Serpinet, J.M. Letoffe, P. Claudy, Chromatographia 22 (1986) 103.
[75] J.W. Menter, D. Tabor, Proc. R. Soc. Lond. A204 (1950) 514.
[76] C. Naselli, J.F. Rabolt, J.D. Swalen, J. Chem. Phys. 82 (1985) 2136.
[77] C. Naselli, J.F. Rabe, J.F. Rabolt, J.D. Swalen, Thin Solid Films 134 (1985) 173.
[78] R.C. Reid, T.K. Sherwood, Properties of Gases and Liquids, McGraw-Hill, New York, 1958.